PHYSICAL REVIEW B VOLUME 42, NUMBER 17 15 DECEMBER 1990-I

Size dependence of electron-phonon coupling in semiconductor nanospheres: The case of CdSe

M. C. Klein, F. Hache, D. Ricard, and C. Flytzanis
Laboratoire d'Optique Quantique du Centre National de la Recherche Scientifique,
Ecole Polytechnique, 91128 Palaiseau CEDEX, France

(Received 2 April 1990)

We study electron-phonon coupling in the case of Fröhlich or polar interaction, with special emphasis on the size dependence of the coupling strength for semiconductor nanospheres exhibiting quantum confinement of the carriers. We first derive the expression of the vibrational LO (longitudinal optic) and SO (surface optic) eigenfunctions for a sphere in the continuum approximation. After having quantized the vibrational eigenmodes, we give the electron-phonon interaction Hamiltonian. Using a model electronic charge distribution, we then show that the coupling strength is size independent when the typical dimensions of the electron charge distribution scale as the sphere radius. These theoretical considerations are then compared with experimental results obtained using resonant Raman scattering by CdSe-doped glasses with particles of various sizes. The experiments confirm the size independence of the coupling strength and also show the existence of surface modes.

I. INTRODUCTION

Electron-phonon coupling is a very important ingredient in determining the physical properties of crystalline materials,[1] for example, in transport processes or in inelastic electron stattering. It is also of relevance in determining the optical properties, both linear and nonlinear, of semiconductors for example. We will concentrate on the case of polar materials such as CdSe for which the dominant coupling is the Fröhlich or polar interaction between the field induced by the vibrational motion and the electronic charge density. In the case of bulk crystals, electron-phonon coupling is now a well-documented effect.[2,3] Following Huang and Rhys,[2] the problem is treated by neglecting anharmonic coupling between phonons in the unperturbed Hamiltonian and by introducing an interaction Hamiltonian linear in the vibrational amplitude. For each eigenmode of wave vector $\mathbf{k}$, the total Hamiltonian can then be exactly diagonalized[3] and the problem is fully equivalent to a shift of a harmonic-oscillator potential whose magnitude is denoted $\Delta_{\mathbf{k}}$, a dimensionless quantity. Neglecting the dispersion of the LO (longitudinal optic) phonon branch, the total coupling is then characterized by[3,4]

$$\Delta^2=\sum_{\mathbf{k}}\Delta_{\mathbf{k}}^2\ ,$$

which is exactly equal to the Huang and Rhys parameter S.

Inelastic electron scattering[5] led to the consideration of semi-infinite materials with a planar interface and of slab-shaped samples.[6–8] In such a case, the internal LO modes are slightly modified and new modes appear: the surface modes. More recently, new materials have been considered: quantum wells,[9] which also belong to the slab-geometry type, and quantum dots,[10] which consist of nearly spherical nanocrystals. The thickness of these quantum wells or the size of the quantum dots is typically a few nanometers. Carrier confinement in one or all three dimensions leads to new optical properties[11–16] which may find important applications in the optical data processing field, thus explaining the intense activity we have recently witnessed in this area.[17–23] In this paper, we will be concerned with quantum dots whose absorption spectra are structured,[13,15] the lowest-energy transition usually being denoted 1*s*-1*s*. The interesting new optical properties are essentially related to condensation of the oscillator strength in these discrete lines.

Electron-phonon coupling may contribute to the broadening of these lines. With this respect, somewhat contradictory results have been published. Using spectral hole burning techniques in the nanosecond domain and CdSe nanospheres, Alivisatos *et al.*[21] find a rather weak coupling ($S\sim0.5$). Using similar techniques in the picosecond domain and similar particles, Roussignol *et al.*[22] find a much stronger coupling ($S\sim2.5$), in agreement with the then available luminescence data.[24] Studying resonant Raman scattering on the same CdSe nanospheres, Alivisatos *et al.*[25] find a much weaker coupling in nanospheres ($S\sim0.5$) than in the bulk ($S\sim10$). A small coupling had also been predicted theoretically for GaAs or InSb quantum dots.[18]

At this point, two comments should be made. First, it is meaningless to compare Raman scattering in the bulk crystal and in nanospheres. In the bulk, $\mathbf{k}$-conservation conditions must be fulfilled, which almost completely forbid first-order scattering[26] and which are gradually relaxed as one goes to higher orders. In the case of nanospheres, where the radius is small compared with the laser wavelength, the dipolar approximation or molecular approach is valid and we are totally free of $\mathbf{k}$ conservation. Second, in the aforementioned papers,[18,22,25] quantum confinement of the phonons was totally neglected. This makes sense when one considers the eigenenergies because of the large ionic masses. However, quantum confinement strongly modifies the eigenfunctions and this, as we will see, has profound consequences on the magnitude of the coupling.

To our knowledge, two other papers have reported on resonant Raman scattering by CdS_xSe_{1-x} nanocrystals. They agree with the small coupling reported by Alivisatos *et al.*[21,25] and clearly show the bimodal behavior of these alloys.[27,28] One of them[28] reports on the excitation spectrum, which roughly corresponds to the 1*s*-1*s* absorption line, while the second one[29] shows evidence of surface phonon modes.

The purpose of the present paper is to study the size dependence of electron-phonon coupling in CdSe nanocrystals, both theoretically and experimentally, using resonant Raman scattering. Experiments are performed on CdSe-doped glasses, but the theoretical considerations are, of course, more general. We will use the same approximations as mentioned in the first part of this Introduction, known as the adiabatic and Condon approximations,[30] and further assume that, for nanospheres, the dominant coupling mechanism is still the polar one. The last assumption is consistent with the fact that these nanospheres are small crystals rather than aggregates. This paper is organized as follows. In Sec. II, we will discuss theoretically the size dependence of electron-phonon coupling in polar semiconductor spheres in the case of Fröhlich interaction where the only relevant modes are the internal LO modes and the surface optic (SO) modes. We will first derive the corresponding eigenfunctions, then give the expression of the interaction Hamiltonian, and finally discuss the size dependence of electron-phonon coupling for a given electronic charge distribution. In Sec. III, we will present resonant Raman experiments performed on CdSe-doped glasses and give the results of this study. These results will be discussed in Sec. IV in the light of the theoretical considerations developed in Sec. II. We will see that the electron-phonon coupling in CdSe nanospheres is size independent, and we discuss the excitation spectrum and the surface modes.

II. THEORY

A. The (LO and SO) vibrational eigenmodes of a semiconductor sphere

In the case of Fröhlich interaction, the only relevant modes are the LO and the surface (SO) modes. We will derive their expression using here the classical macroscopic model. We consider a semiconductor sphere of radius R and dielectric constant ϵ embedded in the surrounding medium of dielectric constant ϵ_d. We neglect any possible anisotropy in ϵ. In the Appendix at the end of this paper, we will show how these models are recovered from the microscopic approach when the surrounding medium is vacuum.

Following Mori and Ando[9] or Licari and Evrard,[8] we start from the standard equations:

$$\mathbf{D}=\epsilon\mathbf{E}=\mathbf{E}+4\pi\mathbf{P} , \tag{1}$$

$$\mathbf{E}=-\nabla\phi , \tag{2}$$

$$\nabla\cdot\mathbf{D}=0 , \tag{3}$$

where $\mathbf{D}$, $\mathbf{E}$, $\mathbf{P}$, and ϕ are the electric displacement, the electric field, the polarization density, and the electric potential, respectively. From Eqs. (1)–(3) we get

$$\epsilon\Delta\phi=0 . \tag{4}$$

Then we have two possibilities. The first one is $\epsilon=0$ and, since the dielectric constant is given by

$$\epsilon(\omega)=\epsilon_\infty\frac{\omega^2-\omega_{\mathrm{LO}}^2}{\omega^2-\omega_{\mathrm{TO}}^2} , \tag{5}$$

where ϵ_∞ is the dielectric constant at high frequency, and ω_{LO} and ω_{TO} are the LO and TO eigenfrequencies related by

$$\frac{\omega_{\mathrm{LO}}^2}{\omega_{\mathrm{TO}}^2}=\frac{\epsilon_0}{\epsilon_\infty} \tag{6}$$

(ϵ_0 is the static dielectric constant), the case $\epsilon=0$ corresponds to the internal LO modes of eigenfrequency ω_{LO}. The eigenfunctions may be written in terms of the orthonormal basis set

$$B_k j_l(kr)Y_l^m(\theta,\varphi) ,$$

where we use spherical coordinates. $j_l(x)$ is the spherical Bessel function of order l and the Y_l^m's are the spherical harmonics. For example, we may write

$$\phi(\mathbf{r})=\sum_{l,m}\sum_k B_k\phi_{l,m}(k)j_l(kr)Y_l^m(\theta,\varphi) , \tag{7}$$

the inverse transform being

$$\phi_{l,m}(k)=\int_{\text{sphere}} B_k\phi(\mathbf{r})j_l(kr)Y_l^{m*}(\theta,\varphi)d\mathbf{r} . \tag{8}$$

The boundary conditions, continuity of ϕ and the normal component of $\mathbf{D}$ at the interface, imply, in the case of the internal LO phonons, that ϕ vanishes outside the sphere and at its surface. We then choose the k's so that for each l,m

$$j_l(kR)=0 . \tag{9}$$

These k's, which depend on l, are then equal to

$$k=\alpha_{n,l}/R , \tag{10}$$

where $\alpha_{n,l}$ is the nth zero of the spherical Bessel function of order l. The true quantum numbers are the n,l,m, but for simplicity we will use the notation l,m,k. Having chosen condition (9), the normalization constant B_k is given by

$$B_k^{-2}=\frac{R^3}{2}j_{l+1}^2(kR) . \tag{11}$$

For $l=0$, this simply reads

$$B_k^2=\frac{2k^2}{R} ,$$

with $k=n\pi/R$ ($n=1,2,3,\ldots$). We then have the expression of ϕ for LO modes and, as we will see, the relative displacement $\mathbf{u}=\mathbf{u}_+-\mathbf{u}_-$ of an ionic pair is proportional to $\mathbf{P}$ and $\mathbf{E}$ and is thus proportional to the gradient of ϕ. Of course, to get physically meaningful results, the quantum numbers must not be too large to account for the finite size of the crystal unit cell.

The second possibility is $\Delta\phi=0$ and this will give us the surface or SO modes. The possible solutions are such that

$$\phi(\mathbf{r})=A_{l,m}r^{l}Y_l^m(\theta,\varphi) \quad \text{for } r<R \ , \tag{12a}$$

$$\phi(\mathbf{r})=B_{l,m}r^{-l-1}Y_l^m(\theta,\varphi) \quad \text{for } r>R \ . \tag{12b}$$

The boundary conditions then imply

$$\epsilon=-\frac{l+1}{l}\epsilon_d \ , \tag{13}$$

with $l=1,2,3,\ldots$. For a given couple (l,m) we have several (as many as R allows) LO modes and only one SO mode. For this mode, once again, $\mathbf{u}$ is proportional to the gradient of ϕ. The eigenfrequencies ω_l must satisfy Eq. (13). In the case of CdSe spheres embedded in glass, the physical constants are given in Table I and we get ω_l values ranging from 194 to 200 cm^{-1} as shown in Table I.

B. Quantization of the eigenmodes and the electron-phonon interaction Hamiltonian

To proceed further, we must calculate the energy or Hamiltonian for a given mode (the free-phonon Hamiltonian). We need the basic equations of the microscopic approach:

$$\mu\ddot{\mathbf{u}}=-\mu\omega_0^2\mathbf{u}+e\mathbf{E}_{\text{loc}} \ , \tag{14}$$

where μ is the reduced mass for an ionic pair and the first term on the right-hand side is the short-range force (we neglect dispersion of the phonon branch), and

$$\mathbf{P}=ne\mathbf{u}+n\alpha\mathbf{E}_{\text{loc}} \ , \tag{15}$$

where n is the number density of pairs and α the polarizability of a pair.

We begin with the LO modes. In our macroscopic approach, the local field is, since $\mathbf{E}=-4\pi\mathbf{P}$,

$$\mathbf{E}_{\text{loc}}=-\frac{8\pi}{3}\mathbf{P} \ , \tag{16}$$

so that, using Eq. (15)

$$\mathbf{P}=\frac{ne}{1+2\beta_{\text{el}}}\mathbf{u} \ , \tag{17}$$

where we use the notation

$$\beta_{\text{el}}=\frac{4\pi}{3}n\alpha \ . \tag{18}$$

TABLE I. Parameters of CdSe-doped glass used to calculate the surface modes eigenfrequencies ω_l. We give the values of the glass dielectric constant, the high-frequency CdSe dielectric constant, the LO and TO phonons eigenfrequencies, and then the calculated values of some ω_l's (for $l=1,2$, and l very large).

ϵ_d	2.25
ϵ_∞	6.1
ω_{LO} (cm^{-1})	210
ω_{TO} (cm^{-1})	170
ω_1 (cm^{-1})	194
ω_2 (cm^{-1})	197
ω_∞ (cm^{-1})	200

Then

$$\nabla\phi=\frac{4\pi ne}{1+2\beta_{\text{el}}}\mathbf{u} \ . \tag{19}$$

For a given mode l,m,k, we start with

$$\mathbf{u}=u_0\nabla j_l(kr)Y_l^m(\theta,\varphi)+\text{c.c.} \tag{20}$$

The kinetic-energy density, for example, is

$$w_c=\tfrac{1}{2}n\mu\dot{\mathbf{u}}^2 \ ,$$

and is integrated over the sphere, the integral being calculated with the use of Green's first identity:[31]

$$\int_V \nabla\phi\cdot\nabla\psi\, d\mathbf{r}=-\int_V \phi\nabla^2\psi d\mathbf{r}+\int_S \phi\frac{\partial\psi}{\partial n}da \ .$$

[In our case, $\phi=\psi\propto j_l(kr)Y_l^m(\theta,\varphi), \nabla^2\psi=-k^2\psi$, and $\phi(r=R)=0$, so that the surface integral vanishes.] We then introduce annihilation and creation operators $a_{lm}(k)$ and $a_{lm}^{\dagger}(k)$ to get the standard Hamiltonian

$$H=\hbar\omega_{\text{LO}}[a_{lm}^{\dagger}(k)a_{lm}(k)+\tfrac{1}{2}] \ . \tag{21}$$

For our l,m,k mode, we thus obtain

$$\mathbf{u}(\mathbf{r})=\left[\frac{\hbar B_k^2}{2n\mu\omega_{\text{LO}}k^2}\right]^{1/2} \times[a_{lm}(k)\nabla j_l(kr)Y_l^m(\theta,\varphi)+\text{H.c.}] \ , \tag{22}$$

where H.c. means Hermitian conjugate. Equations (22) and (19) then give the expression for ϕ, the electric potential:

$$\phi(\mathbf{r})=\frac{4\pi ne}{1+2\beta_{el}}\left[\frac{\hbar B_k^2}{2n\mu\omega_{\text{LO}}k^2}\right]^{1/2} \times[a_{lm}(k)j_l(kr)Y_l^m(\theta,\varphi)+\text{H.c.}] \ , \tag{23}$$

which can be rewritten as

$$\phi(\mathbf{r})=\left[\frac{2\pi\hbar\omega_{\text{LO}}B_k^2}{k^2}\right]^{1/2}\left[\frac{1}{\epsilon_\infty}-\frac{1}{\epsilon_0}\right]^{1/2} \times[a_{lm}(k)j_l(kr)Y_l^m(\theta,\varphi)+\text{H.c.}] \tag{24}$$

since

$$\frac{1}{1+2\beta_{el}}\left[\frac{4\pi ne^2}{\mu\omega_{\text{LO}}^2}\right]^{1/2}=\left[\frac{1}{\epsilon_\infty}-\frac{1}{\epsilon_0}\right]^{1/2} .$$

Considering now all the LO modes, we get the final result

$$\phi(\mathbf{r})=\sum_{l,m}\sum_{k} f_{lm}(k)[a_{lm}(k)j_l(kr)Y_l^m(\theta,\varphi)+\text{H.c}] \ , \tag{25}$$

with

$$f_{lm}(k)=\left[\frac{2\pi\hbar\omega_{\text{LO}}B_k^2}{k^2}\right]^{1/2}\left[\frac{1}{\epsilon_\infty}-\frac{1}{\epsilon_0}\right]^{1/2} . \tag{26}$$

The electron-LO-phonon Hamiltonian then reads

$$H'_{e\text{-ph}}=\int_{\text{sphere}}\phi(\mathbf{r})\rho(\mathbf{r})d\mathbf{r} \ , \tag{27}$$

where $\rho(\mathbf{r})$ is the electronic charge density.

We now proceed to the same calculation for the SO modes. We have

$$\mathbf{E}_{\mathrm{loc}}=\mathbf{E}+\frac{4\pi}{3}\mathbf{P} \tag{28}$$

and, for a given mode of frequency ω_l, eliminating $\mathbf{P}$ between Eqs. (14) and (15), we get

$$\mathbf{E}=(1-\beta_{el})\frac{\mu}{e}(\omega_{\mathrm{TO}}^2-\omega_l^2)\mathbf{u} \ , \tag{29}$$

where we used the relation

$$\omega_{\mathrm{TO}}^2=\omega_0^2-\frac{\omega_p^2}{3(1-\beta_{el})} \ ,$$

with

$$\omega_p^2=\frac{4\pi n e^2}{\mu} \ .$$

The equivalent of Eq. (19) is then

$$\nabla\phi=(1-\beta_{el})\frac{\mu}{e}(\omega_l^2-\omega_{\mathrm{TO}}^2)\mathbf{u} \ . \tag{30}$$

For a given mode l,m, we start now with

$$\mathbf{u}=u_0\nabla r^l Y_l^m(\theta,\varphi)+\text{c.c.} \ , \tag{31}$$

and calculate the energy. We also use Green's first identity, but this time it is the volume integral that vanishes. We introduce the annihilation and creation operators a_{lm}^S and $a_{lm}^{\dagger S}$. For our l,m mode, we thus obtain

$$\mathbf{u}(\mathbf{r})=\left[\frac{\hbar}{2n\mu\omega_l lR}\right]^{1/2}\left[a_{lm}^S\nabla\left[\frac{r}{R}\right]^l Y_l^m(\theta,\varphi)+\text{H.c.}\right] \ . \tag{32}$$

With Eq. (30), this gives for this mode

$$\phi(\mathbf{r})=(1-\beta_{el})\frac{\mu}{e}(\omega_l^2-\omega_{\mathrm{TO}}^2)\left[\frac{\hbar}{2n\mu\omega_l lR}\right]^{1/2}\times\left[a_{lm}^S\left[\frac{r}{R}\right]^l Y_l^m(\theta,\varphi)+\text{H.c.}\right] \ , \tag{33}$$

which, since

$$\epsilon(\omega_l)=-\frac{l+1}{l}\epsilon_d \ ,$$

can be rewritten as

$$\phi(\mathbf{r})=\frac{\sqrt{l}\,\epsilon_\infty}{l\epsilon_\infty+(l+1)\epsilon_d}\omega_{\mathrm{LO}}\left[\frac{2\pi\hbar}{\omega_l R}\right]^{1/2}\left[\frac{1}{\epsilon_\infty}-\frac{1}{\epsilon_0}\right]^{1/2}\times\left[a_{lm}^S\left[\frac{r}{R}\right]^l Y_l^m(\theta,\varphi)+\text{H.c}\right] \tag{34}$$

Considering now all the SO modes, we obtain the final result:

$$\phi(\mathbf{r})=\sum_{l,m}f_{lm}^S\left[a_{lm}^S\left[\frac{r}{R}\right]^l Y_l^m(\theta,\varphi)+\text{H.c}\right] \ , \tag{35}$$

with

$$f_{lm}^S=\frac{\sqrt{l}\,\epsilon_\infty}{l\epsilon_\infty+(l+1)\epsilon_d}\omega_{\mathrm{LO}}\left[\frac{2\pi\hbar}{\omega_l R}\right]^{1/2}\left[\frac{1}{\epsilon_\infty}-\frac{1}{\epsilon_0}\right]^{1/2} \tag{36}$$

and, here also, the electron-SO–phonon Hamiltonian is

$$H''_{e\text{-ph}}=\int_{\text{sphere}}\phi(\mathbf{r})\rho(\mathbf{r})d\mathbf{r} \tag{37}$$

assuming that $\rho(\mathbf{r})$ vanishes outside the sphere.

We now have the electron-phonon Hamiltonian for a sphere, but before proceeding, we check the correctness of our results. Considering a large sphere, we should get the same coupling as with the usual plane-wave decomposition: this coupling should not depend on the shape of the crystal nor on the boundary conditions. Let us consider the same charge density as Merlin *et al.*,[4] consisting of a localized hole and an electron in a hydrogenic state:

$$\rho(\mathbf{r})=\rho_h(\mathbf{r})+\rho_e(\mathbf{r}) \ , \tag{38a}$$

with

$$\rho_h(\mathbf{r})=e\delta(\mathbf{r}) \ , \tag{38b}$$

and

$$\rho_e(\mathbf{r})=-e(\pi a_0^3)^{-1}e^{-2r/a_0} \ , \tag{38c}$$

where a_0 is the exciton Bohr radius. For simplicity, we have located our charge distribution at the center of the sphere but this does not modify the result.

We consider first the plane-wave formalism in which case the potential ϕ is[3]

$$\phi(\mathbf{r})=\sum_{\mathbf{k}}-i\frac{4\pi}{k}\left[\frac{\hbar\omega_{\mathrm{LO}}}{8\pi V}\right]^{1/2}\left[\frac{1}{\epsilon_\infty}-\frac{1}{\epsilon_0}\right]^{1/2}\times(a_{\mathbf{k}}e^{i\mathbf{k}\cdot\mathbf{r}}-\text{H.c.}) \ , \tag{39}$$

where V is the volume of the parallelepiped. Following Duke and Mahan,[3] we introduce

$$v(\mathbf{k})=-i\frac{4\pi}{k}\left[\frac{\hbar\omega_{\mathrm{LO}}}{8\pi V}\right]^{1/2}\left[\frac{1}{\epsilon_\infty}-\frac{1}{\epsilon_0}\right]^{1/2}\int e^{i\mathbf{k}\cdot\mathbf{r}}\rho(\mathbf{r})d\mathbf{r} \ , \tag{40}$$

which allows to calculate the coupling strength $S=\Delta^2$

$$\Delta^2=\sum_{\mathbf{k}}\frac{1}{(\hbar\omega_{\mathrm{LO}})^2}|v(\mathbf{k})|^2 \ . \tag{41}$$

This calculation is performed by Merlin *et al.*[4]

Consider now our sphere with its eigenmodes. For the LO modes, the equivalent of $v(\mathbf{k})$ is

$$v(l,m,k)=f_{lm}(k)\int j_l(kr)Y_l^m(\theta,\varphi)\rho(\mathbf{r})d\mathbf{r} \ . \tag{42}$$

We notice that our radial charge distribution only couples to the $l=0$ LO modes and does not couple to the surface modes. We then have

$$\Delta^2=\sum_k\frac{1}{(\hbar\omega_{\mathrm{LO}})^2}|v(0,0,k)|^2 \ . \tag{43}$$

The calculation is easily performed (we replace $\sum_k$ by $(R/\pi)\int_o^{k_0} dk$ and use the same upper bound as Merlin *et al.*[4] and leads exactly to the same result, namely

$$\Delta^2 = \frac{e^2}{a}\left[\frac{24}{\pi}\right]^{1/3} \frac{1}{\hbar\omega_{\mathrm{LO}}}\left[\frac{1}{\epsilon_\infty} - \frac{1}{\epsilon_0}\right]\frac{1}{w}\int_0^w \frac{x^4(2+x^2)^2}{(1+x^2)^4}dx \tag{44}$$

where $w=(3\pi^2)^{1/2}a_0/a$ and a is the lattice parameter. This proves the correctness of Eqs. (25) and (26).

C. Size dependence of electron-phonon coupling for nanospheres

We now come to the case of semiconductor nanospheres exhibiting quantum confinement and concentrate on the first or 1*s*-1*s* electronic transition. The implications of electron-phonon coupling on this transition depend on the charge density of this excited state. We have an electron and a hole both confined within a spherical box for which one usually assumes infinite walls and interacting through the Coulomb potential. Apart from image field effects, the problem is then similar to that of the helium atom. Using variational techniques, the energy may then be calculated with a high accuracy, but the wave functions are not known. We will therefore assume a model charge distribution.

We will assume that only the electron is confined and that the hole resides at the center of the sphere. More specifically, we have

$$\rho_h(\mathbf{r}) = e\delta(\mathbf{r}) \ , \tag{45a}$$

$$\rho_e(\mathbf{r}) = -e\frac{\pi}{2R^3}j_0^2\left[\frac{\pi r}{R}\right] \quad \text{for } r<R \ , \tag{45b}$$

and

$$\rho(\mathbf{r}) = \rho_h(\mathbf{r}) + \rho_e(\mathbf{r}) = 0 \quad \text{for } r>R \ . \tag{45c}$$

The charge density we assume may not be very realistic, especially concerning the hole, but in the case of CdSe for which only the electronic wave function is quantum confined[32] whereas the hole resides near the center of the sphere,[33] it may be considered as a first approximation.

Here again, we have a radial charge distribution which couples only to the $l=0$ LO modes. We must then calculate $v(0,0,k)$

$$v(0,0,k) = f_{00}(k)\frac{e}{\sqrt{4\pi}} \times \left[1 - \frac{4\pi^2}{2R^3}\int_0^R j_0(kr)j_0^2(k_1 r)r^2 dr\right] \ , \tag{46}$$

where $k=n\pi/R$ and $k_1=\pi/R$. Setting $x=kr$, the second term in the large parentheses reads

$$-2\pi^2\frac{1}{(n\pi)^3}\int_0^{n\pi} j_0(x)j_0^2\left[\frac{x}{n}\right]x^2 dx \ ,$$

and is independent of the radius R of the sphere. The coupling strength Δ^2 is then, using Eqs. (11), (26), and (43), of the form

$$\Delta^2 = \frac{1}{R}\sum_k C_k \ ,$$

where C_k is a constant independent of R. If the sphere is not too small, we may replace $\sum_k$ by $(R/\pi)\int_0^{k_0} dk$, where k_0 depends only on the lattice parameter.

We thus arrive at the conclusion that, for this model charge distribution, the electron-phonon coupling is size independent. From the above calculation, it is clear that the same conclusion would hold for any charge distribution whose typical dimensions scale as the sphere radius R, whether or not it is radial, and then whether or not it is coupled to SO modes. The main conclusion of this section is the following: so long as the charge distribution has typical dimensions scaling as the sphere size, the magnitude of electron-phonon coupling is size independent. This result is intimately related and due to the confinement of the vibrational wave functions, which plays a central role.

We already said in the Introduction that previous papers on electron-phonon coupling in nanospheres did not take phonon confinement into account: the standard plane-wave formalism was used.[18,22,25] Two effects were pointed out however. First, reducing the size of the spheres leads to an increasing overlap of the electron and hole wave functions, implying a decrease of the coupling strength. Second, the same reduction of size should lead to an increasing coupling to short-wavelength phonons. Qualitatively speaking, we may say that we have shown here that these two effects exactly compensate. But this is not predicted by the plane-wave formalism. The correct treatment must take phonon confinement into account and is the one we derived in this section.

III. EXPERIMENTS AND RESULTS

We have performed resonant Raman-scattering measurements on semiconductor-doped glasses (SDG). The scattered light was analyzed by a 75-cm focal length Jarrell-Ash double monochromator and conventional photon-counting techniques were used. As excitation light we used the 4762-, 4825-, 5208-, 5309-, and 5682-Å lines of a cw krypton-ion laser. Most of the experiments were performed at ~77 K using a liquid-nitrogen cryostat; some measurements were performed at room temperature. The output power of the laser was kept below 100 mW and the laser beam was focused to a spot of ~1 mm diameter on the sample, at 40° from normal incidence. The scattered light was collected on the same side of the sample.

Even at these moderate intensities, photodarkening[24] of the SDG was observed, the major effect being a decrease in the luminescence intensity and, as observed by Van Wonterghem *et al.*,[34] photodarkening is at least as easily observed at 77 K as at room temperature.

Figure 1 shows the Raman spectrum obtained at room temperature for a commercial Schott RG 610 filter which contains nanoparticles of an alloy $\mathrm{CdS}_x\mathrm{Se}_{1-x}$. We clearly see the bimodal behavior of these alloys, the first order consisting of two peaks: LO (1) for CdSe around 200

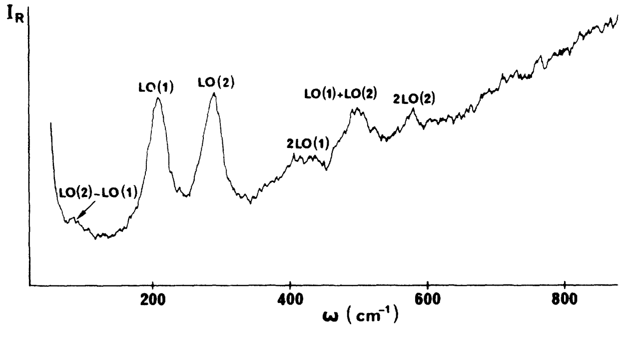

FIG. 1. Resonant Raman spectrum of a Schott RG 610 glass obtained at room temperature with $\lambda_{exc}=5309$ Å. The assignment of the various lines which appear on the rising edge of the luminescence is indicated in the figure and discussed in the text.

cm^{-1} and LO(2) for CdS around 290 cm^{-1}. The second-order spectrum is observable on the rising edge of the luminescence and consists of three peaks: two overtones 2LO(1) and 2LO(2) and a combination tone LO(1)+LO(2). We also see the LO(2)−LO(1) peak. From the relative intensities of the LO(1) and LO(2) peaks, we conclude that the stoichiometric parameter x is ~ 0.3.[27] This value is in agreement with the spin-orbit splitting observed in dc Stark measurements[35] ($\Delta_{SO} \sim 0.33$ eV). The positions of the Raman lines are also in good agreement with this composition. This means that the Schott RG 610 filter contains $CdS_{0.3}Se_{0.7}$ and not $CdS_{0.6}Se_{0.4}$ as written in Ref. 35.

Most of the measurements were performed on CdSe-doped glasses. Figure 2, for example, shows the Raman spectrum obtained for a commercial RG 715 filter at 77 K. The mean particle radius is 40 Å. Four Raman orders are clearly seen with an eigenfrequency of 210 cm^{-1}. In fact, in the melt of RG 715 filters, S and Te are incorporated together with Se,[36] but the Raman spectrum clearly shows that the nanoparticles are essentially CdSe particles. Samples containing particles of various sizes were prepared in the following way. A melt was prepared as for the commercial fabrication of RG 715 filters. When cooled, it is still almost transparent. A bar-shaped sample of this melt is then heat treated in a temperature gradient for 24 or 72 h. Such a bar clearly shows the variation of particle size, the color changing gradually from pale yellow to deep red because of confinement. Samples are then cut in the bar and in our Raman studies, glasses containing particles with a mean radius ranging from 19 to 40 Å were used. These radii were determined from the blue shift of the first absorption peak, which is in good agreement with the theoretical prediction:[37]

$$\Delta E = \frac{\hbar^2\pi^2}{2m_e R^2} , \tag{47}$$

where m_e is the electron mass.

The main object of this study was the size dependence of electron-phonon coupling. Another Raman spectrum is shown in Fig. 3 corresponding to particles of mean radius 20 Å at 77 K. It exemplifies the general trend. At a given temperature and in the size range we studied, the first-order intensity to second-order intensity ratio remains constant within the experimental uncertainty: it is size independent. At 77 K, this ratio is measured to be 2.7±0.1. This first-order intensity to second-order intensity ratio increases when the temperature is increased in agreement with the observations of Alivisatos *et al.*[25] At room temperature, this ratio is ~3.3. Finally, when possible, the five excitation wavelengths were used successively. The aforementioned ratio was observed not to depend significantly on the excitation wavelength.

In Sec. II, we showed that apart from LO modes at 210 cm^{-1} (for CdSe), there exist surface modes whose frequencies range between 194 and 200 cm^{-1}. These surface modes were indeed observed as shown in Fig. 4. In this case, the slit width of the monochromator was reduced, and the surface modes clearly appear as a wing to the first-order LO peak. They also contribute significantly to the second order, with their overtones and probably combination tones.

Finally, using the five lines of the krypton laser, we studied the excitation spectrum of resonant Raman

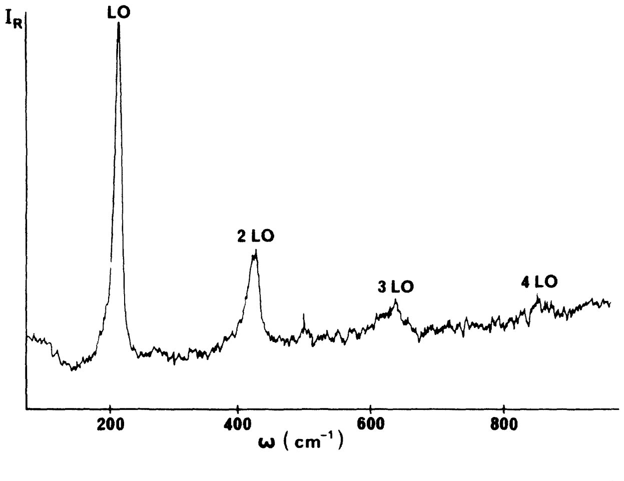

FIG. 2. Resonant Raman spectrum of a Schott RG 715 glass obtained at 77 K with $\lambda_{exc}=5682$ Å. The mean particle radius is 40 Å. Four orders of the CdSe LO mode are visible.

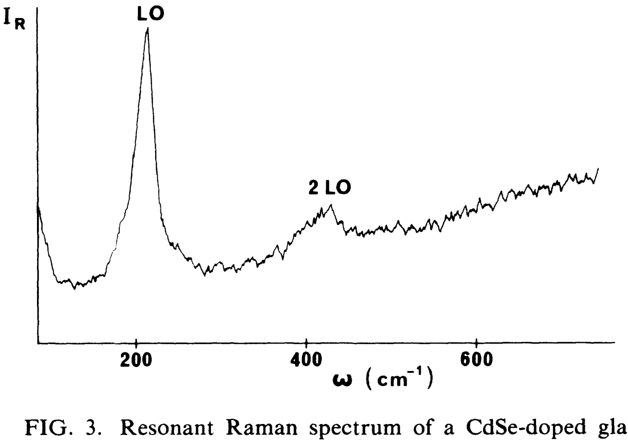

FIG. 3. Resonant Raman spectrum of a CdSe-doped glass obtained at 77 K with $\lambda_{exc}=4825$ Å. The mean particle radius is 19 Å.

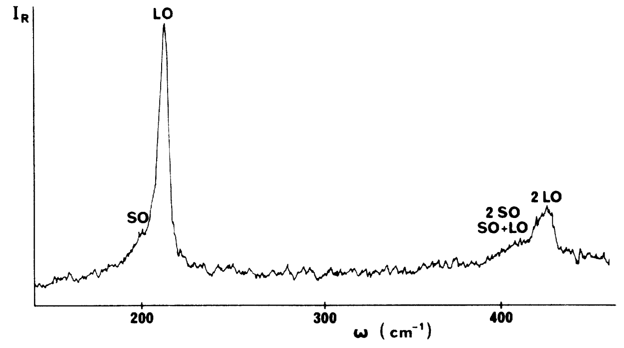

FIG. 4. Resonant Raman spectrum of the same sample as in Fig. 2, also obtained at 77 K with $\lambda_{exc}=5682$ Å. The double-monochromator slits have been closed in order to make the surface phonon modes (indicated by SO) visible.

scattering for these samples. The measurements were performed both at 77 K and at room temperature. The spectral response of the monochromator and photomultiplier tube system was corrected for with the help of the 322-cm^{-1} line of a CaF$_2$ plate and the absorption losses were taken into account in the usual way.[38] A typical result is given in Fig. 5 (at 77 K), showing the absorption spectrum and the excitation efficiency at the five different wavelengths. The already reported[25,28] general trends are recovered: the excitation peaks near the 1*s*-1*s* transition, upper lying states are ineffective in producing resonant Raman scattering. But a new feature is observed: especially at 77 K, the excitation spectrum seems to be red-shifted compared with the 1*s*-1*s* transition. Of course, our five laser lines were too few to draw a definite conclusion for one sample. But this was observed on all the samples we studied.

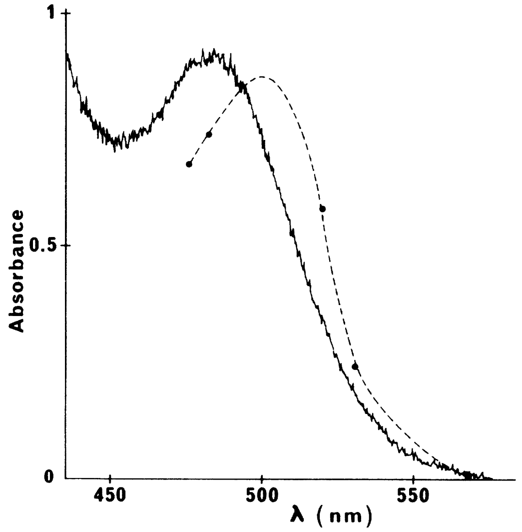

FIG. 5. Absorption spectrum (solid line) and Raman excitation "spectrum" (dots) of the same sample as used in Fig. 3. The temperature is 77 K. The excitation spectrum consists of only five points and is tentatively indicated by the dashed line. The red shift of the excitation spectrum was observed for all samples.

IV. DISCUSSION

The various electron-phonon coupling formalisms (plane waves, slab, sphere) for the LO phonons lead to the same conclusion. The various LO phonons of frequency $\omega_{\rm LO}$ are equivalent to a single vibrational mode, as in the case of a diatomic molecule. For resonant Raman scattering, only two electronic states need be considered: the ground state $|g\rangle$ and the resonant excited state $|e\rangle$. For both electronic states, the vibrational potential curve is assumed to be a parabola with the same curvature, the upper parabola being displaced in the q dimension by the quantity

$$q_0=2\left[\frac{\hbar}{2\mu\omega_{\rm LO}}\right]^{1/2}\Delta\ . \tag{48}$$

(The displacement could just as well be put in the p dimension.) The various formalisms only differ in the way Δ is calculated. We recall that Δ^2 and the Huang and Rhys parameter S are the same thing.

Following Merlin *et al.*[4] and taking the finite temperature into account, the Raman cross section for the nth order line is given by[39]

$$\sigma_n^R=\mu_e^4\sum_{j=0}^{\infty}\left|\sum_{m=0}^{\infty}\frac{\langle g,n+j|e,m\rangle\langle e,m|g,j\rangle}{E_{eg}+(m-j)\hbar\omega_{\rm LO}-\hbar\omega+i\hbar\Gamma}\right|^2 \times\exp(-j\hbar\omega_{\rm LO}/k_BT)\ , \tag{49}$$

where μ_e is the electronic transition dipole moment, $\hbar\omega$ is the incident photon energy, E_{eg} is the (R-dependent) excited-state energy, k_B is Boltzmann's constant, T is the temperature, and notations such as $|e,m\rangle$ or $|g,n\rangle$ denote the mth vibrational state for the excited electronic state and the nth vibrational state for the ground electronic state. Γ is the inverse of the dephasing time T_2.

The overlap integral between the vibrational states is easily calculated:

$$\langle e,n|g,m\rangle=e^{-\Delta^2/2}\sqrt{n!m!}\Delta^{n-m}\times\sum_{j=0}^{m}\frac{(-\Delta^2)^j}{(m-j)!(n-m+j)!j!}$$

when $n\geq m$ and

$$\langle e,m|g,n\rangle=(-1)^{n+m}\langle e,n|g,m\rangle\ .$$

Equation (49) may not perfectly reflect the situation. Since it involves the dephasing time T_2, only off-diagonal elements of the density matrix are taken into account, whereas since the experimental measurements are time integrated, no distinction can be made between Raman scattering and luminescence. Nevertheless, this formalism is a good starting point and we will use Eq. (49) in the following. (The excited state $|e\rangle$ is the 1*s*-1*s* state.) From the Raman cross section σ_n^R for a given size, we calculate the total Raman cross section by taking into account the finite-size dispersion

$$\sigma_n=\int\sigma_n^R p(R)dR\ , \tag{50}$$

assuming for R a Gaussian distribution with a relative size dispersion of $\sim 10\%$. We could instead assume a Gaussian distribution for the energy E_{eg}, but this does not modify the results significantly.

The first-order ($n=1$) intensity to second-order ($n=2$) intensity ratio η then depends only on the values assumed by Γ and Δ. For a given temperature, we may assume Γ to be constant, so that the size independence of this ratio is in complete agreement with the predictions of Sec. II C of a size-independent coupling constant Δ^2. Now, using the same values as Alivisatos *et al.*[25] ($\Gamma=140\ \text{cm}^{-1}$ and $\Delta^2=0.5$), we get good agreement between the measured value of η (2.7 ± 0.1) and the calculated value (2.8) at 77 K. The best value of Δ^2 of course depends on the value we assume for Γ. For example, assuming $\Gamma=200\ \text{cm}^{-1}$, the best agreement is then obtained for $\Delta^2\sim0.9$. However, it seems clear that the value given by Alivisatos *et al.*[21] ($S\sim0.5$) has the correct order of magnitude and that the value inferred by Roussignol *et al.*[22] by assigning the total intrinsic broadening to phonon broadening is too large. Such a small value is in agreement with recent luminescence measurements to be reported independently,[40] which also point to an S value of order 0.5–1. The previously reported luminescence peak[24] is in fact due to trapped carriers.

Assuming again $\Gamma=140\ \text{cm}^{-1}$ and $\Delta^2=0.5$, Eqs. (49) and (50) lead to a decrease of the ratio η when the temperature is increased from 77 K to room temperature. However, the observed increase in η may be accounted for if we assume that Γ increases when the temperature is increased, a quite plausible assumption. Equation (49) therefore adequately reproduces the observations at this point. It predicts, however, a slow and slight decrease of the ratio η as the excitation frequency is tuned from below to above the resonance, a trend which is not unambiguously observed experimentally. But we should take into account the limited accuracy of the measurements and the simplicity of the model, which assumes only one excited state.

In Sec. II, considering spheres, we saw that a radial charge distribution does not couple to the surface modes, whereas surface modes are observed (although weak) experimentally. We first note that they have the predicted eigenfrequencies. We then point to the assumption of the calculation, namely, perfect spheres. Real nanocrystals with diameters ranging from 38 to 80 Å cannot be perfect spheres: this is already forbidden by the crystalline nature of the particles. There is then no surprise in observing coupling between the charge distribution and the surface modes of our imperfect spheres. This is in some respect equivalent to having higher-order charge densities. Nevertheless, we see that the surface modes contribute much more weakly than internal modes to Raman scattering despite the fact that for the smallest nanocrystals, about $\frac{1}{3}$ of the atoms are surface atoms. This supports the conclusions of Sec. II and explains why surface modes are often difficult to observe.[10]

Finally, we will discuss the excitation spectrum, which seems to be, especially at 77 K, slightly red-shifted compared to the 1*s*-1*s* transition. This could be related to the presence of several closely lying excited states. We already have two valence bands (A and B) which lead to two different excited states.[23] But we may also have a third one related to the standard luminescence peak, which is now assigned to trapped carriers. This trapping level may contribute only weakly to the absorption spectrum, but, having a longer lifetime, it may contribute efficiently to resonant Raman scattering. Since these experimental results were obtained with only five laser lines (but several samples with shifted absorption spectra), these considerations are for the time being hypothetical. In fact, what is needed is an excitation spectrum obtained with a continuously tunable dye laser. These experiments are now presently underway.

V. CONCLUSION

In this paper, we first considered theoretically the problem of electron-phonon coupling in (small) semiconductor spheres. We first derived the expressions of the relevant eigenfunctions corresponding to the LO and SO modes; we then gave the coupling Hamiltonian for these two categories of modes, and finally showed that when the charge distribution typical dimensions scale as the sphere radius, the coupling strength S or Δ^2 is constant. We also showed that a radial charge distribution does not couple to the surface modes. Of course, the results depend on the validity of the continuum model we used (this has been discussed by others[9]) and should not be expected to hold for very small spheres where a cluster model would be needed.

We then reported experimental results obtained using resonant Raman scattering by CdSe-doped glasses as a function of particle size, temperature, and excitation wavelength. These results confirm the size independence of electron-phonon coupling in nanospheres. The observation of surface modes is assigned to the fact that our nanocrystals are not perfectly spherical, while the excitation spectrum was tentatively explained in terms of a lower-lying excited state.

These results seem to indicate that, in our CdSe nanocrystals, the typical dimensions of the excited-state charge distribution scale as the radius. One may wonder whether this is a general phenomenon. In the case of GaAs or InSb, it was argued[18] that strong confinement should lead to perfect overlap of the electron and hole wave functions. This may not be the case: of course, the Coulomb energy is negligible when compared with the confinement kinetic energy; however, this does not mean that Coulomb interaction has negligible implications on the wave functions. Only an experimental study of GaAs or InSb quantum dots would settle the question.

As a final comment, we stress that we only compared small CdSe particles with smaller ones and not CdSe nanoparticles with bulk CdSe. We may say, however, that it is generally believed[41] that electron-phonon coupling in bulk CdSe is rather weak (on the order of 0.5–1) so that it is not clear whether S is reduced or not when going from the bulk CdSe crystal to small spheres. We may say that a charge distribution such as that assumed by Merlin *et al.*[4] is rather unrealistic. This comment is, however, outside the scope of the present work, which aimed at comparing small spheres with smaller ones.

ACKNOWLEDGMENTS

We would like to thank Dr. N. Neuroth and Dr. K. E. Remitz from Schott Glaswerke, who prepared the experimental CdSe-doped samples, and Dr. G. Lampel and his co-workers for the loan of their Raman equipment. We also gratefully acknowledge stimulating discussions with J. Hutter.

APPENDIX

We may recover the LO and SO modes of a sphere from the microscopic approach when the sphere is surrounded by vacuum ($\epsilon_d=1$). The starting equations are Eqs. (14) and (15) and the equation giving the local field $\mathbf{E}_{\mathrm{loc}}$. When the sphere is large enough,

$$\mathbf{E}_{\mathrm{loc}}=\frac{4\pi}{3}\mathbf{P}+\mathbf{E}' ,$$

where $\mathbf{E}'(\mathbf{r})$ is the field created at position $\mathbf{r}$ by all the dipoles contained in the sphere. Eliminating $\mathbf{u}$ and $\mathbf{E}_{\mathrm{loc}}$, we arrive at an equation for $\mathbf{P}$. Since we are interested in irrotational solutions, we may set

$$\mathbf{P}=\nabla\phi' \tag{A1}$$

(ϕ' and the true electric potential ϕ are proportional),

$$\delta\nabla_{\mathbf{r}}\phi'(\mathbf{r})=\nabla_{\mathbf{r}}\int_{\mathrm{sphere}}\nabla_{\mathbf{r}'}\frac{1}{|\mathbf{r}-\mathbf{r}'|}\cdot\nabla_{\mathbf{r}'}\phi'(\mathbf{r}')d\mathbf{r}' , \tag{A2}$$

where, following the notations of Licari and Evrard,[8]

$$\delta=\frac{(\lambda-\lambda_0)(1-\beta_{el})+4\pi/3}{1-n\alpha(\lambda-\lambda_0)} . \tag{A3}$$

The integral in Eq. (A2) is evaluated using Green's first identity, leading to

$$\delta\nabla_{\mathbf{r}}\phi'(\mathbf{r})=\nabla_{\mathbf{r}}\left[\int_{\mathrm{surf}}\phi'(\mathbf{r}')\frac{\partial}{\partial n'}\frac{1}{|\mathbf{r}-\mathbf{r}'|}da' -\int_{\mathrm{sphere}}\phi'(\mathbf{r}')\nabla^2\frac{1}{|\mathbf{r}-\mathbf{r}'|}d\mathbf{r}'\right] . \tag{A4}$$

For a given (l,m) couple, and for $r'>r$,

$$\frac{1}{|\mathbf{r}-\mathbf{r}'|}=\frac{4\pi}{2l+1}\frac{r^l}{r'^{\,l+1}}Y_l^m(\theta,\varphi)Y_l^{m*}(\theta',\varphi') . \tag{A5}$$

Setting $\phi'(\mathbf{r})=\phi'(r)Y_l^m(\theta,\varphi)$, the surface integral is

$$I_s=-4\pi\frac{l+1}{2l+1}\phi'(R)\frac{r^l}{R^l}Y_l^m(\theta,\varphi) . \tag{A6}$$

Then, since $\Delta 1/|\mathbf{r}-\mathbf{r}'|=-4\pi\delta(\mathbf{r}-\mathbf{r}')$, the volume integral is

$$I_V=-4\pi\phi'(\mathbf{r}) . \tag{A7}$$

Equation (A4) then becomes

$$(\delta-4\pi)\nabla_{\mathbf{r}}\phi'(r)Y_l^m(\theta,\varphi) =-4\pi\frac{l+1}{2l+1}\phi'(R)\nabla_{\mathbf{r}}\left[\frac{r}{R}\right]^l Y_l^m(\theta,\varphi) . \tag{A8}$$

There are two possibilities: the first one is

$$\phi'(R)=0 , \tag{A9a}$$

$$\delta=4\pi , \tag{A9b}$$

and, since a little algebra shows that

$$\frac{4\pi}{\delta}-1=-\epsilon(\omega) , \tag{A10}$$

we have $\omega=\omega_{\mathrm{LO}}$ and recover the LO modes.

The second case corresponds to:

$$\phi'(R)\neq 0 , \tag{A11a}$$

so that

$$\delta-4\pi\neq 0 , \tag{A11b}$$

leading to

$$\phi'(\mathbf{r})=-4\pi\frac{l+1}{2l+1}\frac{1}{\delta-4\pi}\phi'(R)\left[\frac{r}{R}\right]^l Y_l^m(\theta,\varphi) . \tag{A12}$$

Equation (A12) for $r=R$ leads to

$$\delta=4\pi\frac{l}{2l+1} , \tag{A13}$$

or, using (A10),

$$\epsilon(\omega)=-\frac{l+1}{l} , \tag{A14}$$

and we recover the SO modes.

---

[1] C. Kittel, *Quantum Theory of Solids* (Wiley, New York, 1967).

[2] K. Huang and A. Rhys, Proc. R. Soc. London Ser. A **204**, 406 (1950).

[3] C. B. Duke and G. D. Mahan, Phys. Rev. **139**, A1965 (1965).

[4] R. Merlin, G. Güntherodt, R. Humphreys, M. Cardona, R. Suryanarayanan, and F. Holtzberg, Phys. Rev. B **17**, 4951 (1978).

[5] H. Boersch, J. Geiger, and W. Stickel, Phys. Rev. Lett. **17**, 379 (1966).

[6] R. Fuchs and K. L. Kliewer, Phys. Rev. **140**, 2076 (1965).

[7] A. A. Lucas, E. Kartheuser, and R. G. Badro, Phys. Rev. B **2**, 2488 (1970).

[8] J. J. Licari and R. Evrard, Phys. Rev. B **15**, 2254 (1977).

[9] N. Mori and T. Ando, Phys. Rev. B **40**, 6175 (1989).

[10] R. Ruppin, J. Phys. C **8**, 1969 (1975).

[11] D. S. Chemla and D. A. B. Miller, J. Opt. Soc. Am. B **2**, 1155 (1985).

[12] Al. L. Efros and A. L. Efros, Fiz. Tekh. Poluprovodn. **16**, 1209 (1982) [Sov. Phys. Semicond. **16**, 772 (1982)].

[13] A. I. Ekimov and A. A. Onushchenko, Pis'ma Zh. Eksp. Teor. Fiz. **40**, 337 (1984) [JETP Lett. **40**, 1137 (1984)].

[14] L. E. Brus, J. Chem. Phys. **80**, 4403 (1984).

[15] R. Rossetti, R. Hull, J. M. Gibson, and L. E. Brus, J. Chem. Phys. **82**, 552 (1985).

[16] H. Weller, H. M. Schmidt, U. Koch, A. Fojtik, S. Baral, A. Henglein, W. Kunath, K. Weiss, and E. Dieman, Chem.

Phys. Lett. **124**, 557 (1986).

[17] A. Henglein, A. Kumar, E. Janata, and H. Weller, Chem. Phys. Lett. **132**, 133 (1986).

[18] S. Schmitt-Rink, D. A. B. Miller, and D. S. Chemla, Phys. Rev. B **35**, 8113 (1987).

[19] Yu. V. Vandyshev, V. S. Dneprovskii, A. I. Ekimov, D. K. Okorokov, L. B. Popova, and Al. L. Efros, Pis'ma Zh. Eksp. Teor. Fiz. **46**, 393 (1987) [JETP Lett. **46**, 495 (1987)].

[20] D. W. Hall and N. F. Borrelli, J. Opt. Soc. Am. B **5**, 1650 (1988).

[21] A. P. Alivisatos, A. L. Harris, N. J. Levinos, M. L. Steigerwald, and L. E. Brus, J. Chem. Phys. **89**, 4001 (1988).

[22] R. Roussignol, D. Ricard, C. Flytzanis, and N. Neuroth, Phys. Rev. Lett. **62**, 312 (1989).

[23] N. Peyghambarian, B. Fluegel, D. Hulin, A. Migus, M. Joffre, A. Antonetti, S. W. Koch, and M. Lindberg, IEEE J. Quantum Electron. **25**, 2516 (1989).

[24] P. Roussignol, D. Ricard, J. Lukasik, and C. Flytzanis, J. Opt. Soc. Am. B **4**, 5 (1987); M. Tomita, T. Matsumoto, and M. Matsuoka, J. Opt. Soc. Am. B **6**, 165 (1989).

[25] A. P. Alivisatos, T. D. Harris, P. J. Carroll, M. L. Steigerwald, and L. E. Brus, J. Chem. Phys. **90**, 3463 (1989).

[26] S. A. Permogorov, A. N. Reznitskii, Ya. V. Morozenko, and B. A. Kazennov, Fiz. Tverd. Tela (Leningrad) **16**, 2403 (1974) [Sov. Phys.—Solid State **16**, 1562 (1975)].

[27] M. Hayek and O. Brafman, in *Light Scattering in Solids*, edited by M. Balkanski (Flammarion, Paris, 1971).

[28] A. V. Baranov, Ya. S. Bobovich, and V. I. Petrov, Opt. Spektrosk. **65**, 1066 (1988) [Opt. Spectrosc. (USSR) **65**, 628 (1988)].

[29] F. Zhou, Y. Sun, and J. Pan, J. Lumin. **40 & 41**, 739 (1988).

[30] G. F. Neumark and K. Kosai, in *Semiconductors and Semimetals*, edited by R. K. Willardson and A. C. Beer (Academic, New York, 1983).

[31] J. D. Jackson, *Classical Electrodynamics* (Wiley, New York, 1975), p. 41.

[32] A. I. Ekimov and Al. L. Efros, Phys. Status Solidi B **150**, 627 (1988).

[33] A. I. Ekimov, A. A. Onushchenko, S. K. Shumilov, and Al. L. Efros, Pis'ma Zh. Tekh. Fiz. **13**, 281 (1987) [Sov. Tech.—Phys. Lett. **13**, 115 (1987)].

[34] B. Van Wonterghem, S. M. Saltiel, T. E. Dutton, and P. M. Rentzepis, J. Appl. Phys. **66**, 4935 (1989).

[35] F. Hache, D. Ricard, and C. Flytzanis, Appl. Phys. Lett. **55**, 1504 (1989).

[36] N. Neuroth (private communication).

[37] P. Roussignol, Ph.D. thesis, Université Paris XI 1989 (unpublished).

[38] R. Loudon, J. Phys. (Paris) **26**, 677 (1965).

[39] P. M. Champion, G. M. Korenowski, and A. C. Albrecht, Solid State Commun. **32**, 7 (1979).

[40] M. C. Klein, F. Hache, D. Ricard, and C. Flytzanis (unpublished).

[41] C. Benoît à la Guillaume (private communication).